



Article

# Histomorphology of Chorionic Villi of Term Placentae of Mothers Exposed to Retroviral and Hepatitis B Viruses

John Ahenkorah <sup>1,†</sup>, Stephen Opoku-Nyarko <sup>1,†</sup>, Kevin Kofi Adutwum-Ofosu <sup>1</sup>, Bismarck Hottor <sup>1</sup>, Joana Twasam <sup>2</sup>, Emmanuel Afutu <sup>2</sup>, Clement Nyadroh <sup>2</sup>, Fleischer C. N. Kotey <sup>2,3</sup>, Eric S. Donkor <sup>2</sup>, Nicholas T. K. D. Dayie <sup>2</sup>, Edem M. A. Tette <sup>4,\*</sup> and Patience B. Tetteh-Quarcoo <sup>2,\*</sup>

- <sup>1</sup> Department of Anatomy, University of Ghana Medical School, Accra P.O. Box KB 4236, Ghana; jahenkorah@ug.edu.gh (J.A.); stevrose91@gmail.com (S.O.-N.); kadutwum-ofosu@ug.edu.gh (K.K.A.-O.); bahottor@gmail.com (B.H.)
- <sup>2</sup> Department of Medical Microbiology, University of Ghana Medical School, Accra P.O. Box KB 4236, Ghana; jtwasam3@gmail.com (J.T.); emmalineafutu@yahoo.com (E.A.); cenyadroh001@st.ug.edu.gh (C.N.); fcnkotey@flerholiferesearch.com (F.C.N.K.); ericsdon@hotmail.com (E.S.D.); ntkddayie@ug.edu.gh (N.T.K.D.D.)
- <sup>3</sup> FleRhoLife Research Consult, Teshie, Accra P.O. Box TS 853, Ghana
- <sup>4</sup> Department of Community Health, University of Ghana Medical School, Accra P.O. Box KB 4236, Ghana
- \* Correspondence: ematette@ug.edu.gh (E.M.A.T.); patborket2002@yahoo.com (P.B.T.-Q.); Tel.: +233-546-159-610 (E.M.A.T.); +233-244-633-251 (P.B.T.-Q.)
- † These authors contributed equally to this work.

**Abstract:** Retroviral and hepatitis B infections can be potential threats to foetomaternal health through inducing distortions of the architecture and structure of the placenta. Improved insights into the effects of these infections on placental morphology would be integral to our understanding of maternal and neonatal health. Aim: To histomorphologically and stereologically investigate selected placental structures in virus-infected (HIV [human immunodeficiency virus] and hepatitis B virus [HBV]) and uninfected women at term. Method: This cross-sectional study involved the screening of 237 placentae collected at term ( $38 \pm 2$  weeks) from the maternity delivery units and surgical theatres of the LEKMA and Weija/Gbawe Municipal Hospitals in Accra. Venous blood samples from the umbilical vein and placenta basal plate blood were screened for HIV, HBV, and hepatitis C virus (HCV) using serological test kits (RDT). A total of 34 placentae were selected, comprising 20 cases and 14 controls that were gestational age-matched. Using stereology and a systematic random sampling technique with test point and intersection counting of photomicrographs, the mean volume densities of syncytial knots, syncytial denudations, foetal capillaries, and intervillous spaces of the placentae were estimated on a total of 2720 photomicrographs. Results: On stereological assessment, there was a statistically significant difference in the mean volume densities of syncytial knots (HIV-infected =  $0.562 \pm 0.115$ , HBV-infected =  $0.516 \pm 0.090$ , control group =  $0.171 \pm 0.018$ ,  $p = 0.001$ ), syncytial denudations (HIV-infected =  $0.121 \pm 0.022$ , HBV-infected =  $0.111 \pm 0.016$ , control group =  $0.051 \pm 0.00$ ,  $p = 0.004$ ), and foetal capillaries (HIV-infected =  $0.725 \pm 0.152$ , HBV-infected =  $0.902 \pm 0.078$ , control group =  $0.451 \pm 0.064$ ,  $p = 0.006$ ) among the different groups of placentae (control) at term. A statistically significant decrease in intervillous space ( $p = 0.022$ ) was recorded in HBV-infected placentae compared to the control (from  $15.450 \pm 1.075$  to  $11.32 \pm 0.952$ ). Conclusion: Placental viral infections might lead to significant increases in syncytial knots, foetal capillaries, and syncytial denuded areas of the chorionic villi and a significant decrease in intervillous spaces. This finding could signify evidence of advanced gestation, placental malperfusion, hypermaturity of the placenta, and a possible vertical transmission of the viral antigen to the foetus, which may be crucial in understanding perinatal outcomes.

**Keywords:** histomorphology; placentae; stereology; syncytial knots; retroviral; hepatitis B



**Citation:** Ahenkorah, J.; Opoku-Nyarko, S.; Adutwum-Ofosu, K.K.; Hottor, B.; Twasam, J.; Afutu, E.; Nyadroh, C.; Kotey, F.C.N.; Donkor, E.S.; Dayie, N.T.K.D.; et al. Histomorphology of Chorionic Villi of Term Placentae of Mothers Exposed to Retroviral and Hepatitis B Viruses. *Acta Microbiol. Hell.* **2024**, *69*, 29–40. <https://doi.org/10.3390/amh69010005>

Academic Editor: Athanassios Tsakris

Received: 12 January 2024

Revised: 5 February 2024

Accepted: 8 February 2024

Published: 26 February 2024



**Copyright:** © 2024 by the authors. Licensee MDPI, Basel, Switzerland. This article is an open access article distributed under the terms and conditions of the Creative Commons Attribution (CC BY) license (<https://creativecommons.org/licenses/by/4.0/>).

## 1. Introduction

Pregnant women are susceptible to a variety of infections, including those caused by viruses such as human immunodeficiency virus (HIV) and hepatitis B virus (HBV), both of which can infect various cellular components of the placenta and be transmitted to the foetus [1]. These infections are a particularly significant public health concern during pregnancy due to their association with foetal malformation and pregnancy complications, such as preterm labour and low birth weight, as well as maternal and neonatal deaths [2–4]. While a number of studies have focused on the transmission of these viral infections from mother to foetus, there is limited data on the effects of these pathogens on placental chorionic villi. Despite a few morphological changes reported in placenta studies, the stereological quantification of these structural changes caused by viral infections in term placentae has not been adequately researched.

Pregnancy-associated complications may be a result of infections contracted during the period of the pregnancy which could adversely affect the structure and histomorphology of the chorionic villi. The chorionic villi are the site of exchange of nutrients, gases, and wastes between the mother and the foetus. Therefore, any damage to the chorionic villi can affect the function of placental barrier structures (e.g., syncytiotrophoblast, cytotrophoblast, trophoblast basement membrane, and foetal capillary endothelium). A better understanding of the effects of infections and the impact of these pathogens on chorionic villi structures in term placentae will improve our understanding in the changes these pathogens can cause to the histomorphology of the placenta barrier.

One of the common methods of investigation to determine the factors endangering the foetus and newborn is examination of the placenta. Therefore, it is essential to ascertain the effects of these infections on the placenta to establish baseline data for understanding the structure of the placenta when infected during pregnancy, which could help in explaining adverse foetal outcomes. The first choice for converting two-dimensional profiles into three dimensions is stereology [5]. It provides a set of clear sampling criteria and a straightforward estimating tool that makes it possible to derive 3D quantities from 2D images that appear on slice planes, such as total and average volumes, surfaces, lengths, and numbers [6]. The quantitative description of morphology is made possible by contemporary stereology and design-based approaches [5]. It has proven to be quite useful for dispelling old myths about how to interpret growth, morphogenesis, adaptation, and functioning at the level of the complete organ when applied to placentae in normal and abnormal pregnancies [7]. Despite the substantial public health significance of placental viral infection, its effects on placental histomorphology are not fully understood. To manage other pregnant mothers and their children effectively, it is essential to understand how infections affect term placentae chorionic villi. A typical method for locating potential dangers to the foetus and baby is to examine how infections affect the placenta. Thus, this study investigated, via stereology, the histomorphology of HIV- and HBV-infected placenta in comparison with normal-term placentae.

## 2. Materials and Methods

### 2.1. Study Design, Site and Sampling

The study was cross-sectional and was carried out at two hospitals in the Greater Accra Region of Ghana—the LEKMA Hospital and the Weija-Gbawe Municipal Hospital. The LEKMA Hospital is located within Ledzokuku Municipality and has about 80 beds. It primarily caters to the health needs of residents of the Municipality and also serves as a referral centre for residents in nearby municipalities, such as La Dadekotokong and Tema West Municipalities. It offers services spanning across diagnostics, emergencies, paediatric care, herbal medicine, surgery, eye care, ENT (ear, nose, and throat), outpatient care, as well as ante-natal and maternal care, etc. and records an average of about 400 births each month. The Weija-Gbawe Municipal Hospital, which offers services similar to those of LEKMA Hospital, is a 70-bed capacity district hospital located in MacCarthy Hills and offers referral services to those residing within the environs of Weija and Gbawe. It records

an average of about 300 births each month. Both hospitals are Government-owned, are under the purview of the Ghana Health Service, run a 24-h service, and have among their referrals most health and pregnancy complicated cases.

A total of two hundred and thirty-seven (237) term placentae were collected from the Obstetrics and Gynaecology Departments of the hospitals and were screened for HIV, HBV, and hepatitis C virus (HCV) using serological test kits (RDT). About 2 to 3 mL of blood from the maternal side (basal plate) as well as cord blood from the umbilical vein on the foetal side of the placenta was collected and kept in well-labelled K<sub>2</sub>EDTA tubes. Blood from maternal circulation (venous blood) was also drawn and kept in labelled K<sub>2</sub>EDTA tubes. All blood samples were subjected to rapid diagnostic testing (RDT) for HIV, HBV, and hepatitis C virus (HCV), after which they were categorised as cases (study group) or controls. The study groups were made up of placenta samples that were found to have been exposed to any of the selected viruses (HIV and HBV; none of the samples was positive for HCV), whereas the control group comprised placenta samples that tested negative for HIV, HBV, and HCV, with matched gestational ages. A total of 34 placentae were selected, comprising 20 cases (10 HIV-positive and 10 HBV-positive) and 14 controls that were gestational age-matched. The inclusion criteria were placentae from pregnant women who delivered in the hospital either by spontaneous vaginal delivery (SVD) or Caesarian section and placentae delivered at full term ( $38 \pm 2$  weeks). However, placentae from pregnant women who delivered with macerated placentae, preterm births, and spontaneous abortions were excluded from the study.

### 2.2. Rapid Diagnostic Test (RDT) for HBV, HCV, and HIV

As per the manufacturer's instructions, a drop of placenta-derived blood was placed on the sample column of the immunoblot test kit (Immunetics Inc., Boston, MA, USA). Four drops of lysing buffer were then added, and the results were compared to the control band and interpreted as RDT-positive (for HIV, HBV, and HCV) or -negative. These RDT kits have high specificities and sensitivities: HIV (specificity = 99.96%; sensitivity = 100%), HBV (specificity = 99.3%; sensitivity = 96.2%), and HCV (specificity = 97.51%; sensitivity = 96.67%).

### 2.3. Slicing and Processing of Tissues

Placenta samples of about 2 cm × 2 cm × 5 cm dimensions taken from the chorionic plate to the basal plate were obtained from the cases (study group) and controls for histopathological studies. The sampling was standardised and involved division of the placenta with the tissue samples taken from the cord area into four equal quadrants until finally reaching the periphery. Each sample was put into a well-labelled tissue cassette and fixed in 10.0% phosphate-buffered formalin of pH 7.24–7.2 to prevent autolysis and ensure proper fixation of tissue before the processing of placental samples.

Each tissue-containing tissue cassette was placed in an automated tissue processor (LEICA TP 1020) with 12 chambers and dehydrated through graded series of increasing concentrations of ethanol (from 70.0% through to 95.0%). The placenta tissues were further dehydrated with steps of absolute alcohol after which two changes of xylene were used for an hour each for clearing. Afterward, the labelled tissues were infiltrated with molten wax (58 °C) embedding medium and allowed to cool to form blocks, ready for microtome sectioning. Each placental tissue sample from each quadrant was embedded in one wax block. After about 18–20 h, the tissue processing was completed.

### 2.4. Sectioning of Placenta Tissue and Staining

Using a Leica microtome (Leica RM 2125, Wetzlar, Germany), the wax-blocked placental tissues were initially trimmed by sectioning at a thickness of 10 µm (m) in order to expose the entire tissue profile. The tissues were then sectioned into slices that were 5 µm thick each, and four of these sections (1st, 50th, 100th, and 150th) were systematically chosen and

stained with hematoxylin and eosin (H&E). For one placenta, a total of 16 slices were taken and placed on a glass slide (76 mm × 26 mm × 1 mm) for histomorphometrical studies.

## 2.5. Stereological Investigations

### 2.5.1. Sampling of Photomicrographs of Placentae Sections

Photomicrographs from a bright-field binocular light microscope were produced by connecting an optical light compound microscope (Leica Galen III, catalogue e no. 317506, serial no. 1125DP) with a digital microscope eyepiece (Lenovo Q350 USB PC Camera) to a desktop computer (HP Compaq dx2300 Microtower). The stage of the Leica Galen III microscope was moved three graduation units on the X and Y axes. The microscope stage was moved from one plane on the X-axis to a different plane on the Y-axis. Photomicrographs of fields of view under the microscope as determined by movements on the X and Y axes were captured using a ×40 objective lens with a camera (Lenovo Q350 USB PC Camera). These movements were repeated till the whole area of the placenta section was covered. The average number of micrographs taken was fifty (50) per placental slide. Micrographs obtained using the sixteen (16) sections per placenta tissue were pooled together and five (5) photomicrographs were selected using systematic uniform random sampling, in which every tenth (10th) photomicrograph was selected from the first randomly selected photomicrograph for stereological studies. A total of eighty (80) micrographs were selected systematically per placenta tissue.

In all, a total of two thousand seven hundred and twenty (2720) photomicrographs were selected systematically for point counting in the stereological grid (Figure 1). A snapshot of the microscope graticule was taken at the same magnification. The micrograph of the graticule was used for calibrating the grid which was used for the stereological study (Figure 2). The sections stained with H&E were used for counting syncytial knots, syncytial denudated areas of the placental villi, foetal capillaries, and intervillous spaces.

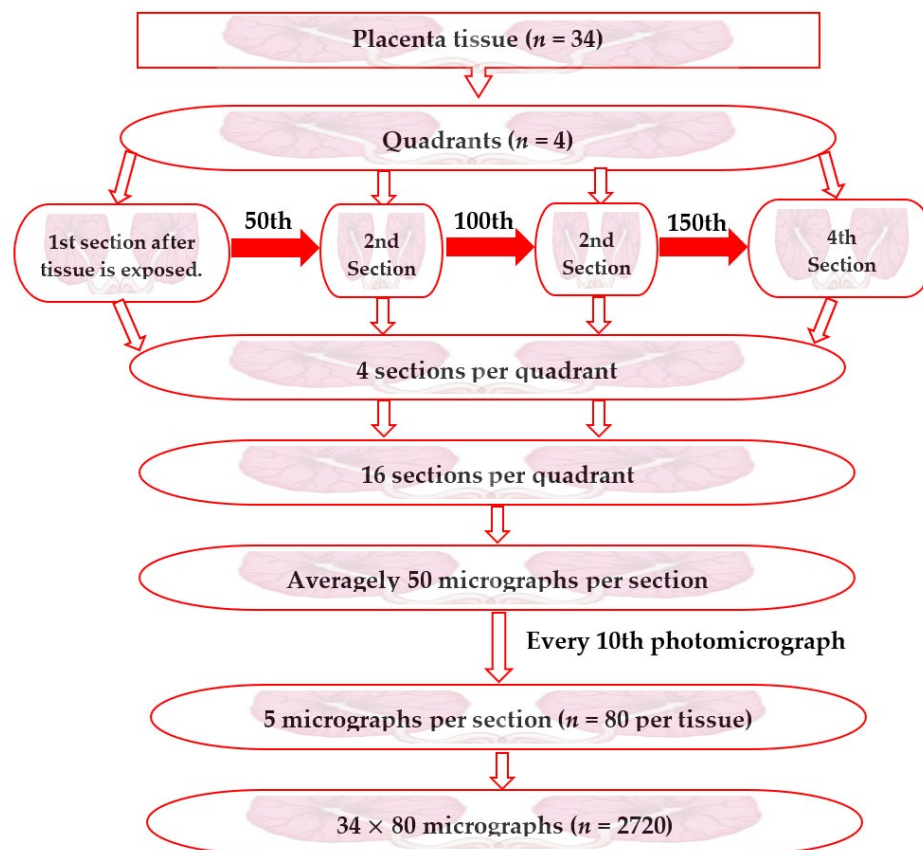


**Figure 1.** Flow chart for stereological systematic random sampling.

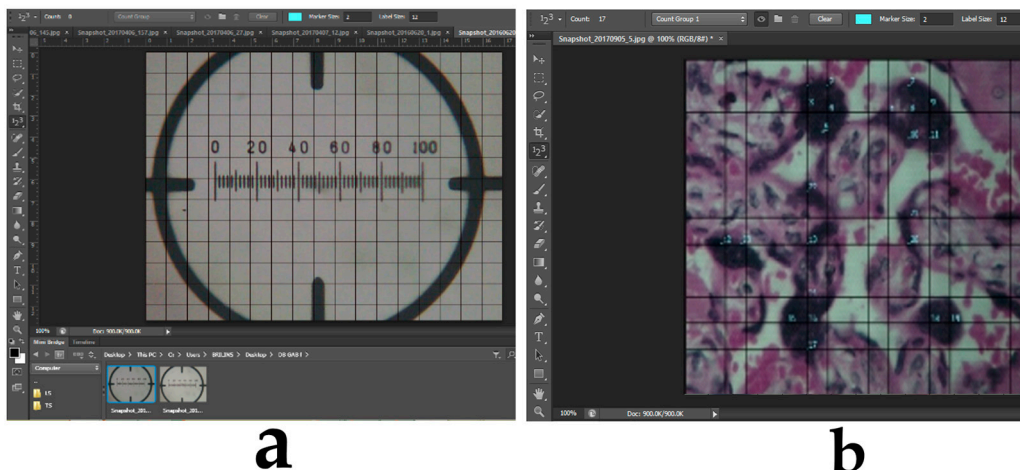


**Figure 2.** Stereological assessment of placental photomicrograms: (a) calibration of the grid using Photoshop; (b) syncytial knot point using Adobe Photoshop.

### 2.5.2. Stereological Examination of Placental Photomicrographs

A design-based stereological method was employed to determine the relative volume densities of various structural variables of the placenta using Cavalieri's principle of point counting. A stereological grid  $1\text{cm} \times 1\text{cm}$  in dimensions consisting of uniformly spaced points in Adobe Photoshop CS6 Extended (trial version 13.0.1) software was superimposed on each micrograph of the placenta section sampled as described above. The desired parameters, namely volume density of syncytial denudations, villi syncytial knots, intervillous spaces, and fetal capillaries, were counted on the micrographs at the point of intersection of the grid lines. Values from the point counting were entered into the formula (Cavalieri estimator of volume) below for the calculation of relative volume densities.

$$Vv = \frac{\sum P \times \left(\frac{a}{p}\right) \times t}{M^2}$$

where  $Vv$  represents volume density,  $\sum P$  is the sum of all test points encountered,  $\left(\frac{a}{p}\right)$  is the area per point of the stereological grid,  $t$  is the thickness of the section, and  $M$  is linear magnification.

### 2.6. Statistical Analysis

Data were entered using Microsoft Excel 2019 (version 16, Microsoft Corporation, Washington, DC, USA) and analysis was conducted using GraphPad Prism software (Version 5, Graphpad Software LLC of Boston, MA, USA). All results are expressed as means, standard deviations (SDs), or standard errors of the means (SEMs), as well as 95% confidence intervals (CIs) for means. One-way analysis of variance and  $t$ -tests were used to compare means within and between the placenta groups.  $p$  values that were less than 0.05 were considered statistically significant. The test for homogeneity of variance was done using Bartlett's test of equality of variances.

### 2.7. Ethical Consideration

This study was approved and given clearance by the Ethical and Protocol Review Committee of the College of Health Sciences, University of Ghana, with protocol identification number CHS-Et/M5-5.6/2019-2020. Participation in the study was made absolutely voluntary and the participants were given the liberty to withdraw from the study without suffering any consequences. Informed consent was also sought from the pregnant women who delivered in the hospital before including their placentae in the study.

### 3. Results

The differences between the mean volume densities were statistically significant (higher) between the placental groups (Table 1).

**Table 1.** Volume density (Vd) of placental parameters in the various placental groups.

Placental Groups	Placental Parameters			
	Syncytial Knots	Intervillous Space	Syncytial Denudation	Foetal Capillaries
Control ( <i>n</i> = 14)	0.171 ± 0.018	15.450 ± 1.075	0.051 ± 0.00	0.451 ± 0.064
HIV ( <i>n</i> = 10)	0.562 ± 0.115 **	12.830 ± 0.826	0.121 ± 0.022 **	0.725 ± 0.152
HBV ( <i>n</i> = 10)	0.516 ± 0.090 **	11.32 ± 0.952 *	0.111 ± 0.016 *	0.902 ± 0.078 **
<i>p</i> value	0.001	0.022	0.004	0.006

Values are shown as mean ± SEM (standard error of the mean) with *p* values representing the level of significance for one-way analysis of variance (followed by Tukey's post hoc) for between-group comparison with \* = *p* < 0.050 and \*\* = *p* < 0.010 compared to the control.

The mean volume densities of the foetal capillaries recorded a statistically significant difference (*p* = 0.006) between the placenta groups (Table 1). Post hoc analysis indicated a statistically significant increase in foetal capillaries in the HBV-infected placenta group compared to the mean volume density of the control group (Figure 3A). However, the increase in foetal capillaries in the HIV-infected placenta group was not statistically significant.

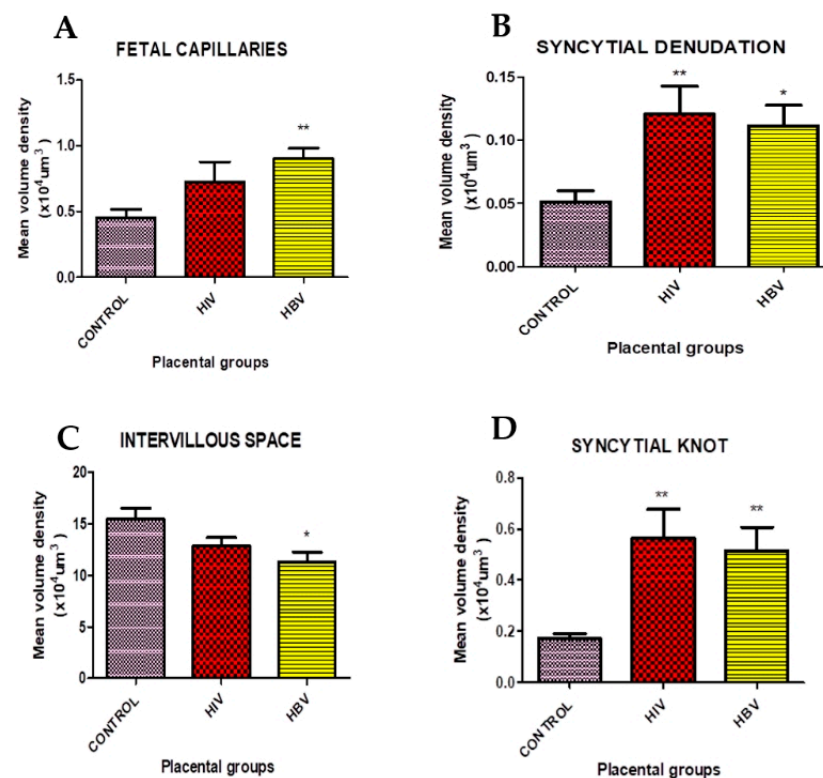


**Figure 3.** Unpaired *t*-test analysis of term placental parameters, comparing healthy (control), HIV-infected, and hepatitis-infected placentae (study group). (A). Volume density of foetal capillaries. (B) Volume density of syncytial denudation. (C) Volume density of intervillous space. (D) Volume density of syncytial knots. Values are expressed as mean ± SEM. *p* values represent significance levels for unpaired T test for time course assessment for the term group comparisons, with \* = *p* < 0.05 and \*\* = *p* < 0.01.

Syncytial denudation, as shown in Table 1, indicates a statistically significant difference (*p* = 0.004) in volume densities. A statistically significant difference in the denudation

of the syncytium was present in the HIV-infected placenta group compared to the control group (Figure 3B). HBV-infected placentae also showed a statistically significant increase in denudated areas of the syncytium of the placenta compared with the control. Also, there was a statistically significant decrease in intervillous space mean volume density for HBV-infected placentae compared to the control group (Figure 3C). The HIV-infected group also had some level of reduction; nonetheless, these reductions were not statistically significant (Table 1). The analysis of volume densities indicated a significant difference ( $p = 0.022$ ) (Table 1). Analysis of variance for the volume density of syncytial knots revealed a significant difference ( $p = 0.001$ ) at a 5.0% chance of error (Table 1). There was also a statistically significant increase in the syncytial knot of both the HIV- and HBV-infected placentae, compared to the control, with a mean volume density of  $0.171 \pm 0.018$  (Figure 3D).

With regard to the histomorphological assessment of HIV and HBV-infected placentae, some varying degrees of syncytial knots (clumps of syncytiotrophoblast nuclei) as shown in Figure 4 (with asterisks) were observed where the numbers were significantly higher in all the viral infected placentae (HIV, HBV) compared with the controls. However, the integrity of the syncytium was generally maintained in the control compared to the HIV- and HBV-infected placentae. Syncytial denudation, which is the shaving away of the syncytium of the placental villi (as shown with curvy lines in Figure 5), was observed in higher quantities in all virus-infected placentae compared to the controls. The number of foetal capillaries in HBV-infected placentae also recorded a high count microscopically compared to the control.

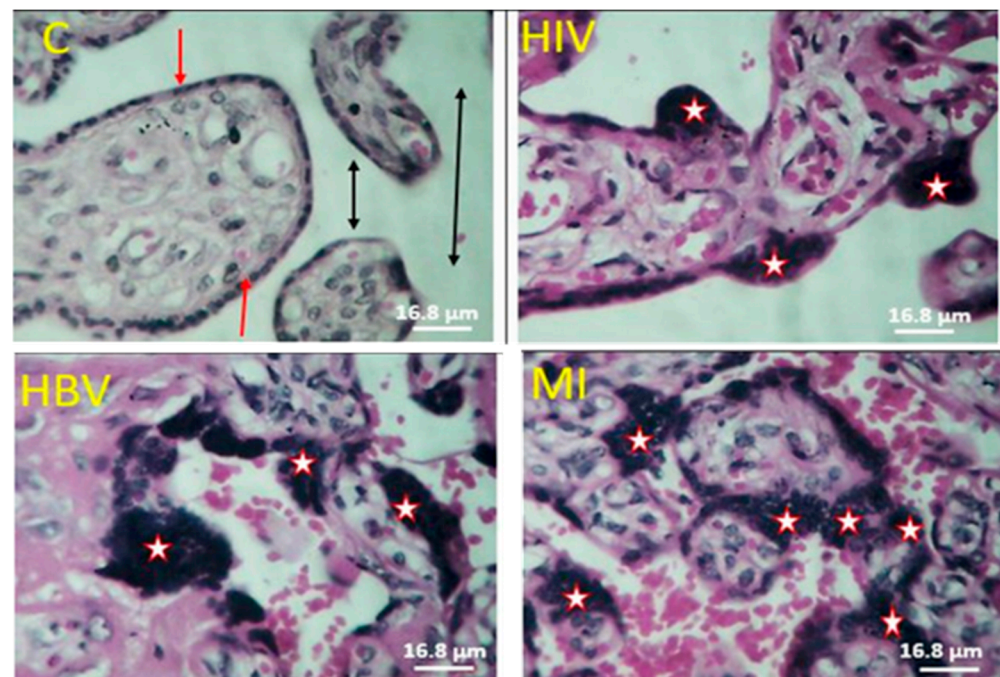


**Figure 4.** Histomorphological appearance of infected placentae showing syncytial knots stained with H&E. (C) shows a normal syncytium. Red-headed arrows and double black-headed arrows show a normal syncytium and intervillous spaces in the control; asterisks indicate syncytial knot formation in HIV-infected, HBV-infected, and mixed-infected (HIV and HBV) placentae, respectively.

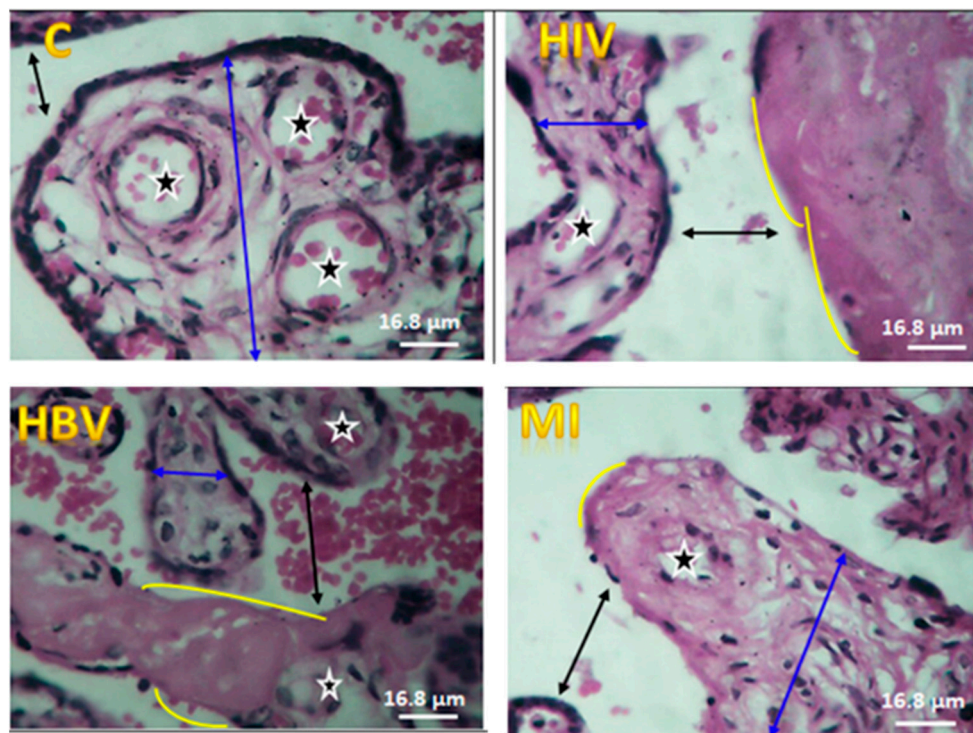


**Figure 5.** Histomorphological appearance of virus-infected placentae showing syncytial denuded areas stained with H&E. Blue double-headed arrows show the villi; asterisk indicates foetal capillaries; black double-headed arrows indicate intervillous spaces. (C) shows a normal syncytium and yellow curvy lines indicate syncytial denuded areas in HIV-, HBV-, and mixed-infected (HIV and HBV) placentae, respectively.

#### 4. Discussion

The purpose of this study was to investigate, via stereology, the histomorphology of selected HIV- and HBV-infected placentae in comparison with normal placentae at term, focusing on syncytial knots, intervillous space, syncytial denudation, and foetal capillaries. Regarding syncytial knot formation, a statistically significant increase was observed among HIV- and HBV-infected placentae compared to the controls, which could be attributed to a number of factors. For example, infection with these viruses may lead to oxidative stress, which eventually culminates in apoptotic and/or necrotic events at the syncytium. Chan et al. [1] and Salmani et al. [8] reported that a significant increase in syncytial knots in the placental villi signifies a disruption in hormonal factors that may contribute to impaired blood flow. Syncytiotrophoblast nuclei morphology is variable and is seen to be condensed, which is reminiscent of apoptotic nuclei [9–11]. This has led to the hypothesis that nuclear aggregation reflects an aging process of the placenta or hyper-maturation [12,13]. Some studies have shown that syncytial nuclei aggregates (SNAs) or syncytial knots are increased in pregnancy complications including reduced foetal movements, pre-eclampsia, maternal diabetes mellitus, intrauterine growth restrictions (IUGR), and still birth compared with normal pregnancies, which is consistent with the present study of viral infections [14–18]. A study conducted by Ahenkorah et al. [19] also revealed a significant increase in syncytial knot formation in placentae infested with *Plasmodium falciparum* compared to normal placentae at term. The authors attributed this increase to the possible blocking of spiral arterioles by infected erythrocytes, which may lead to oxidative stress and syncytium apoptotic events. The result of this present study is in agreement with the findings of Bentley-Lewis et al. [20] and Heorman et al. [21], in whose studies increased syncytial knots were found in the placentae of diabetic mothers. The significant increase in the knotting in these studies was attributed to reduced foetal villus blood flow and to premature aging of the placenta as part of the pathophysiology of diabetes [22].

Concerning syncytial denudation, HIV-infected placentae had a significantly higher volume density of villous syncytial denuded areas. This may be suggestive of changes in the villus syncytiotrophoblast layer, which may have been caused by the viral infection itself and/or even the use of antiretroviral drugs [23]. In this study, it has been shown that the structural integrity of the placenta–blood barrier may have been greatly compromised, and hence the significantly higher volume densities of the denuded areas in virus-infected placentae. Although maternal immune cells do not cross this barrier, interestingly, maternal immunoglobulins (Ig), including IgG, further contribute to intrauterine immune defence [24]. However, in light of this finding, it has been revealed that viral particles might cross to the foetal side of the placenta through the denuded areas of the placental villi all the way into cord blood. Since the foetomaternal barrier may have been breached through syncytial denudation, blood from intervillous spaces may seep directly into the chorionic villi and subsequently into the foetal capillaries, thereby transmitting any infection present to the foetus. Mayhew et al. [25] reported that hypoxia *in vitro* stimulates cytotrophoblast proliferation but inhibits recruitment into the syncytiotrophoblast, and this could account for the long-lasting non-replacement of denuded syncytiotrophoblast nuclei, leaving the villi exposed to infections. Similarly, Huppertz et al. [26] demonstrated that cytotrophoblast proliferation is inversely related to oxygen tension, thus supporting earlier findings in both the villus trophoblast and in the extravillous cytotrophoblast [27,28]. Under hypoxic conditions, cytotrophoblast accumulation, in tandem with the breakdown of the overlying syncytiotrophoblast, is indirect evidence of the absence of syncytial fusion [29]. A study conducted by Alsat et al. [30] has shown that isolated primary trophoblast cells show reduced fusion under hypoxia compared to normoxia *in vitro*, especially in diseased conditions. This reduced fusion under hypoxia is further supported by immunochemical data from Huppertz et al. [26], in whose study several proteins transcribed exclusively in the cytotrophoblast (e.g., Bcl-2, cascade 3) were no longer found in the syncytiotrophoblast, but rather accumulated in the cytotrophoblast. The time of infection is relevant to finding histopathological alterations in the placenta, especially with respect to denuded areas of the villus syncytium. In our case, this is difficult to conclude, since the time of infection was not the scope of this study. A further study comparing an early infection in the first trimester to a late infection in the third trimester would be interesting with regard to syncytial denuded areas. Structural alterations in term placentae were consistent with the findings reported in those studies [31,32].

Foetal capillaries were significantly increased in the study group compared to the controls in the current study. This was observed in the villi of HIV- and HBV-infected placentae where the mean volume densities of foetal capillaries increased but were statistically significant and more pronounced in HBV-infected placentae compared with the control in this study. The presence of excess blood vessels in the placental villi is referred to as chorangiogenesis. According to the pertinent literature, chorangiogenesis is associated with having an enlarged placenta, maternal diabetes, and immature villi [33,34]. It has been noted in the literature that chorangiogenesis is also associated with smoking, twin gestations, delivery at high altitudes, and maternal anaemia. In a study by Akbarzadeh-Jahromi et al. [35], the authors stated that previous abortion and intrauterine insemination (IUI) could be considered the cause since they can create hypoperfused areas in the uterus. The numerous and enlarged foetal capillaries in the placental villi in disease conditions compared with the controls may be the placenta's response to foetal distress, which might produce numerous foetal capillaries in order to receive oxygen and nourishment for the developing foetus.

Regarding intervillous spaces, the decrease in volume density was statistically significant among HBV-infected placentae when compared with the controls. Kingdom [36] reported that an unusually wide intervillous space combined with abnormally small villus calibres is a usual finding in post-placental hypoxia. That study is contrary to what was observed in this study but consistent with a study by Rainey and Mayhew [37] which reported that IUGR was in correlation with significantly lower intervillous space, villi volumes, and decreased villi surface area, suggesting that these dimensions are isometric.

Villous maldevelopment in IUGR has been shown to be correlated with changes in estimated number and size of intervillous pores and the estimated number of villus domain [37]. Intervillous pores and villus domains are not conventional architectural units but geometric constructs that define local point-sampled areas, considered an arbitrary space. Intervillous space, considered to be the potential volume through which oxygen molecules could pass to reach the villus trophoblast surface, relies not only on the total size of intervillous space but also on the number, size, and spatial arrangement of villus trees within it. This reduction in volume density of intervillous spaces may also be caused by the intermittent expulsion of maternal blood loss resulting from uterine wall placenta detachment [38]. This decrease could also be a result of villous congestion or excess proliferation which may lead to hypoxic events leading to foetal death or preterm labour. This decrease in IVS could also be associated with HIV- and HBV-infected placentae in this study, although earlier studies have shown that intervillous pore volumes increase with umbilical arterial pressure during pregnancy, in the placentae of women who are heavy smokers, and those who were raised and completed their pregnancies at higher altitudes [39–41]. However, this study cannot extrapolate its findings in this regard, although it has been reported in other studies that changes in the shapes of intervillous pores are influenced by changes in the sizes and spatial arrangement of villus trees [42,43]. The structural alterations observed in this study regarding syncytial knot formation, foetal capillaries, syncytial denuded areas, and the decrease in volume density of intervillous spaces in HIV- and HBV-infected placentae are the key findings of this study.

## 5. Conclusions

Human immunodeficiency virus and hepatitis B infections during pregnancy have adverse effects on the internal architecture of the placenta which could possibly explain perinatal outcomes. Our findings consolidate existing insights that HIV and hepatitis B viral infections may cause a significant increase in syncytial knot formation. This could signify a hypermaturation of chorionic villi, with syncytial denudations signifying a breach of the foetomaternal placental barrier and foetal capillaries. It also indicates a possible cause of chorangiomas as a result of a probable hypoxic condition and a decrease in intervillous space, which could signify villous congestion or excess proliferation.

**Author Contributions:** Conceptualisation, J.A. and P.B.T.-Q.; data curation, P.B.T.-Q., J.A., S.O.-N., J.T., K.K.A.-O., C.N., B.H. and N.T.K.D.D.; formal analysis, P.B.T.-Q., J.A., S.O.-N., J.T., F.C.N.K., E.S.D. and E.A.; investigation, P.B.T.-Q., S.O.-N., J.A., C.N. and N.T.K.D.D.; methodology, P.B.T.-Q., E.A., J.A., S.O.-N., E.M.A.T. and J.T.; project administration, P.B.T.-Q., E.M.A.T. and J.A.; resources, P.B.T.-Q., E.A., J.A., C.N., K.K.A.-O., B.H., E.M.A.T. and E.S.D.; software, P.B.T.-Q., E.A., S.O.-N., J.A. and F.C.N.K.; supervision, P.B.T.-Q. and J.A.; validation, P.B.T.-Q., E.M.A.T. and J.A.; visualisation, P.B.T.-Q., J.A., E.A., F.C.N.K., N.T.K.D.D., B.H. and K.K.A.-O.; writing—original draft, P.B.T.-Q., J.A., S.O.-N., J.T., F.C.N.K., N.T.K.D.D., E.S.D., E.A. and K.K.A.-O.; and writing—review and editing, P.B.T.-Q., E.A., S.O.-N., J.T., F.C.N.K., N.T.K.D.D., J.A., B.H., C.N., E.M.A.T. and K.K.A.-O. All authors have read and agreed to the published version of the manuscript.

**Funding:** This research received no external funding.

**Institutional Review Board Statement:** This study was conducted in accordance with the Declaration of Helsinki and approved by the Ethics and Protocol Review Committee of the College of Health Sciences with Protocol Identification Number CHS-Et/M5-5.6/2019-2020.

**Informed Consent Statement:** Informed consent was sought from pregnant women who delivered in the hospitals before including their placentae in this study.

**Data Availability Statement:** The data presented in this study are available on reasonable request from the corresponding authors.

**Acknowledgments:** The authors wish to thank all the members of staff of the Departments of Medical Microbiology and Anatomy (UGMS) as well as the staff of the LEKMA Hospital and the Weija-Gbawe Municipal Hospital of the Greater Accra Region for their immense support during sample collection. We also acknowledge Peter Ofori Appiah for his contribution during the writing process.

**Conflicts of Interest:** The authors declare no conflicts of interest.

## References

- Chan, M.Y.; Smith, M.A. Infections in Pregnancy. *Compr. Toxicol.* **2018**, *8*, 232–249. [CrossRef]
- Cardenas, I.; Means, R.E.; Aldo, P.; Koga, K.; Lang, S.M.; Booth, C.; Manzur, A.; Oyarzun, E.; Romero, R.; Mor, G. Viral Infection of the Placenta Leads to Foetal Inflammation and Sensitization to Bacterial Products Predisposing to Preterm Labor. *J. Immunol.* **2010**, *185*, 1248–1257. [CrossRef]
- Mor, G.; Cardenas, I.; Abrahams, V.; Guller, S. Inflammation and pregnancy: The role of the immune system at the implantation site. *Ann. N. Y. Acad. Sci.* **2011**, *1221*, 80–87. [CrossRef] [PubMed]
- Agrawal, V.; Hirsch, E. Intrauterine infection and preterm labor. *Semin. Fetal Neonatal Med.* **2012**, *17*, 12–19. [CrossRef] [PubMed]
- Ochs, M.; Schipke, J. A short primer on lung stereology. *Respir. Res.* **2021**, *22*, 305. [CrossRef] [PubMed]
- Altunkaynak, B.Z.; Onger, M.E.; Altunkaynak, M.E.; Ayranci, E.; Canan, S. A brief introduction to stereology and sampling strategies: Basic concepts of stereology. *NeuroQuantology Interdiscip. J. Neurosci. Quantum Phys.* **2012**, *10*, 31. Available online: <https://link.gale.com/apps/doc/A485671454/AONE?u=anon~b320218b&sid=googleScholar&xid=53f9f1d5> (accessed on 18 February 2023). [CrossRef]
- Mayhew, T.M.; Sisley, I. Quantitative studies on the villi, trophoblast and intervillous pores of placentae from women with well-controlled diabetes mellitus. *Placenta* **1998**, *19*, 371–377. [CrossRef] [PubMed]
- Salmani, D.; Purushothaman, S.; Somashekara, S.C.; Gnanagurudasan, E.; Sumangaladevi, K.; Harikishan, R.; Venkateshwarareddy, M. Study of structural changes in placenta in pregnancy-induced hypertension. *J. Nat. Sci. Biol. Med.* **2014**, *5*, 352–355. [CrossRef] [PubMed]
- Burton Graham, J.; Jones, C.J.P. Syncytial knots, sprouts, apoptosis, and trophoblast deportation from the human placenta. *Taiwan. J. Obstet. Gynecol.* **2009**, *48*, 28–37. [CrossRef] [PubMed]
- Burton, G.J. Deportation of syncytial sprouts from the term human placenta. *Placenta* **2011**, *32*, 96–98. [CrossRef]
- Sharp, A.N.; Heazell, A.E.P.; Baczyk, D.; Dunk, C.E.; Lacey, H.A.; Jones, C.J.P.; Perkins, J.E.; Kingdom, J.C.P.; Baker, P.N.; Crocker, I.P. Preeclampsia is associated with alterations in the p53-pathway in villous trophoblast. *PLoS ONE* **2014**, *9*, e87621. [CrossRef]
- Sharp, A.N.; Heazell, A.E.P.; Crocker, I.P.; Mor, G. Placental apoptosis in health and disease. *Am. J. Reprod. Immunol.* **2010**, *64*, 159–169. [CrossRef] [PubMed]
- Coleman, S.; Gerza, L.; Jones, C.; Sibley, C.; Aplin, J.; Heazell, A. Syncytial nuclear aggregates in normal placenta show increased nuclear condensation, but apoptosis and cytoskeletal redistribution are uncommon. *Placenta* **2013**, *34*, 449–455. [CrossRef] [PubMed]
- Heazell, A.E.P.; Moll, S.J.; Jones, C.J.P.; Baker, P.N.; Crocker, I.P. Formation of Syncytial Knots is Increased by Hyperoxia, Hypoxia and Reactive Oxygen Species. *Placenta* **2007**, *28*, S33–S40. [CrossRef] [PubMed]
- Bamfo, J.E.A.K.; Odibo, A.O. Diagnosis and management of foetal growth restriction. *J. Pregnancy* **2011**, *2011*, 640715. [CrossRef] [PubMed]
- Warrander, L.K.; Batra, G.; Bernatavicius, G.; Greenwood, S.L.; Dutton, P.; Jones, R.L.; Sibley, C.P.; Heazell, A.E.P. Maternal perception of reduced foetal movements is associated with altered placental structure and function. *PLoS ONE* **2012**, *7*, e34851. [CrossRef] [PubMed]
- Heazell, A. The placenta and adverse pregnancy outcomes—Opening the black box? *BMC Pregnancy Childbirth* **2015**, *15*, 14–15. [CrossRef]
- Pollock, D.; Ziaian, T.; Pearson, E.; Cooper, M.; Warland, J. Breaking through the silence in antenatal care: Foetal movement and stillbirth education. *Women Birth* **2020**, *33*, 77–85. [CrossRef] [PubMed]
- Ahenkorah, J.; Tetteh-Quarcoo, P.B.; Nuamah, M.A.; Kwansa-Bentum, B.; Nuamah, H.G.; Hottor, B.; Korankye, E.; Torto, M.; Ntumy, M.; Addai, F.K. The Impact of *Plasmodium* Infection on Placental Histomorphology: A Stereo-logical Preliminary Study. *Infect. Dis. Obstet. Gynecol.* **2019**, *2019*, 2094560. [CrossRef]
- Bentley-Lewis, R.; Dawson, D.L.; Wenger, J.B.; Thadhani, R.I.; Roberts, D.J. Placental histomorphometry in gestational diabetes mellitus: The relationship between subsequent type 2 diabetes mellitus and race/ethnicity. *Am. J. Clin. Pathol.* **2014**, *141*, 587–592. [CrossRef]
- Gheorman, L.; Pleşea, I.E.; Gheorman, V. Histopathological considerations of placenta. *Rom. J. Morphol. Embryol.* **2012**, *53*, 329–336. [PubMed]
- Benirschke, K.; Burton, G.J.; Baergen, R.N. *Pathology of the Human Placenta*, 6th ed.; Springer: Berlin/Heidelberg, Germany, 2012; pp. 1–941. [CrossRef]

23. Baurakiades, E.; Martins, A.P.C.; Moreschi, N.V.; Souza, C.D.A.; Abujamra, K.; Saito, A.O.; Mecatti, M.C.; Santos, M.G.; Pimentel, C.R.; Silva, L.L.G.; et al. Histomorphometric and immunohistochemical analysis of infectious agents, T-cell subpopulations and inflammatory adhesion molecules in placentas from HIV-seropositive pregnant women. *Diagn. Pathol.* **2011**, *6*, 101. [[CrossRef](#)] [[PubMed](#)]
24. Schneider, H.; Miller, R.K. Receptor-mediated uptake and transport of macromolecules in the human placenta. *Int. J. Dev. Biol.* **2010**, *54*, 367–375. [[CrossRef](#)] [[PubMed](#)]
25. Mayhew, T.M.; Bowles, C.; Yücel, F. Villous trophoblast growth in pregnancy at high altitude. *J. Anat.* **2002**, *200*, 533. [[CrossRef](#)]
26. Huppertz, B.; Kingdom, J.; Caniggia, I.; Desoye, G.; Black, S.; Korr, H.; Kaufmann, P. Hypoxia Favours Necrotic Versus Apoptotic Shedding of Placental Syncytiotrophoblast into the Maternal Circulation. *Placenta* **2003**, *24*, 181–190. Available online: <http://linkinghub.elsevier.com/retrieve/pii/S0143400402909033> (accessed on 5 March 2023). [[CrossRef](#)]
27. Caniggia, I.; Mostachfi, H.; Winter, J.; Gassmann, M.; Lye, S.J.; Kuliszewski, M.; Post, M. Hypoxia-inducible factor-1 mediates the biological effects of oxygen on human trophoblast differentiation through TGF $\beta$ <sub>3</sub>. *J. Clin. Investig.* **2000**, *105*, 577–587. [[CrossRef](#)] [[PubMed](#)]
28. Kosanke, G.; Kadyrov, M.; Korr, H.; Kaufmann, P. Maternal anemia results in increased proliferation in human placental villi. *Placenta* **1998**, *19*, 339–357. [[CrossRef](#)]
29. Fox, H. Effect of hypoxia on trophoblast in organ culture. A morphologic and autoradiographic study. *Am. J. Obstet. Gynecol.* **1970**, *107*, 1058–1064. [[CrossRef](#)]
30. Alsat, E.; Wyplosz, P.; Malassiné, A.; Guibourdenche, J.; Porquet, D.; Nessmann, C.; Evain-Brion, D. Hypoxia impairs cell fusion and differentiation process in human cytotrophoblast, in vitro. *J. Cell. Physiol.* **1996**, *168*, 346–353. [[CrossRef](#)]
31. Aliota, M.T.; Caine, E.A.; Walker, E.C.; Larkin, K.E.; Camacho, E.; Osorio, J.E. Characterization of Lethal Zika Virus Infection in AG129 Mice. *PLoS Negl. Trop. Dis.* **2016**, *10*, e0004682. [[CrossRef](#)]
32. Seferovic, M.D.; Turley, M.; Valentine, G.C.; Rac, M.; Castro, E.C.C.; Major, A.M.; Sanchez, B.; Eppes, C.; Sanz-Cortes, M.; Dunn, J.; et al. Clinical importance of placental testing among suspected cases of congenital zika syndrome. *Int. J. Mol. Sci.* **2019**, *20*, 712. [[CrossRef](#)] [[PubMed](#)]
33. Ogino, S.; Redline, R.W. Villous capillary lesions of the placenta: Distinctions between chorangioma, chorangiomatosis, and chorangiosis. *Hum. Pathol.* **2000**, *31*, 945–954. [[CrossRef](#)] [[PubMed](#)]
34. Dureau, Z.J.; Rogers, B.B. Placental pathology. *Diagn. Histopathol.* **2019**, *25*, 341–349. [[CrossRef](#)]
35. Akbarzadeh-Jahromi, M.; Soleimani, N.; Mohammadzadeh, S. Multiple chorangioma following long-term secondary infertility: A rare case report and review of pathologic differential diagnosis. *Int. Med. Case Rep. J.* **2019**, *12*, 383–387. [[CrossRef](#)] [[PubMed](#)]
36. Kingdom, J.C.K.P. Oxygen and placental vascular development. *Hypoxia Next Millenn.* **1999**, *474*, 259–275.
37. Rainey, A.; Mayhew, T. Volumes and Numbers of Intervillous Pores and Villous Domains in Placentas Associated with Intrauterine Growth Restriction and/or Pre-eclampsia. *Placenta* **2010**, *31*, 602–606. [[CrossRef](#)] [[PubMed](#)]
38. Dellschaft, N.S.; Hutchinson, G.; Shah, S.; Jones, N.W.; Bradley, C.; Leach, L.; Platt, C.; Bowtell, R.; Gowland, P.A. The haemodynamics of the human placenta in utero. *PLoS Biol.* **2020**, *18*, e3000676. [[CrossRef](#)] [[PubMed](#)]
39. Karimu, A.L.; Burton, G.J. Star volume estimates of the intervillous clefts in the human placenta: How changes in umbilical arterial pressure might influence the maternal placental circulation. *J. Dev. Physiol.* **1993**, *19*, 137–142. [[PubMed](#)]
40. Mayhew, T.; Wadrop, E. Placental morphogenesis and the star volumes of villous trees and intervillous pores. *Placenta* **1994**, *15*, 209–217. [[CrossRef](#)]
41. Mayhew, T.; Brotherton, L.; Holliday, E.; Orme, G.; Bush, P. Fibrin-type fibrinoid in placentae from pregnancies associated with maternal smoking: Association with villous trophoblast and impact on intervillous porosity. *Placenta* **2003**, *24*, 501–509. [[CrossRef](#)]
42. Mayhew, T.M. A stereological perspective on placental morphology in normal and complicated pregnancies. *J. Anat.* **2009**, *215*, 77–90. [[CrossRef](#)]
43. Plitman Mayo, R. Advances in Human Placental Biomechanics. *Comput. Struct. Biotechnol. J.* **2018**, *16*, 298–306. [[CrossRef](#)]

**Disclaimer/Publisher’s Note:** The statements, opinions and data contained in all publications are solely those of the individual author(s) and contributor(s) and not of MDPI and/or the editor(s). MDPI and/or the editor(s) disclaim responsibility for any injury to people or property resulting from any ideas, methods, instructions or products referred to in the content.